Hydrological Processes

WILEY

RESEARCH ARTICLE

Spatial Variation of Changes in Extreme Discharge Seasonality Across the Northeastern United States

Owen H. Richardson[1] | Carl E. Renshaw[1] | Francis J. Magilligan[2]

[1]Department of Earth Sciences, Dartmouth College, Hanover, New Hampshire, USA | [2]Department of Geography, Dartmouth College, Hanover, New Hampshire, USA

Correspondence: Owen H. Richardson (owen.richardson@colostate.edu)

Received: 28 May 2024 | **Revised:** 6 September 2024 | **Accepted:** 11 October 2024

Funding: This work was partially funded by the National Science Foundation (BCS-1626414 and BCS-1951469), the Mellam Family Foundation Research Award, the Neukom Institute for Computational Science and the Dartmouth College Department of Earth Sciences.

Keywords: climate warming | extreme flooding | extreme precipitation

ABSTRACT

The Northeast United States exhibits significant spatial heterogeneity in flood seasonality, with spring snowmelt-driven floods historically dominating northern areas, while other regions show more varied flood seasonality. While it is well documented that since 1996 there has been a marked increase in extreme precipitation across this region, the response of flood seasonality to these changes in extreme precipitation and the spatial distribution of these effects remain uncertain. Here we show that, historically, snowmelt-dominated northern regions were relatively insensitive to changes in extreme precipitation. However, with climate warming, the dominance of snowmelt floods is decreasing and thus the extreme flood regimes in northern regions are increasingly susceptible to changes in extreme precipitation. While extreme precipitation increased everywhere in the Northeastern United States in 1996, it has since returned to near pre-1996 levels in the coastal north while remaining elevated in the inland north. Thus, the inland north region has and continues to experience the greatest changes in extreme flooding seasonality, including a substantial rise in floods outside the historical spring flood season, particularly in smaller watersheds. Further analysis reveals that while early winter floods are increasingly common, the magnitude of cold season floods (Nov-May) have remained unchanged over time. In contrast, warm season floods (June-Oct), historically less significant, are now increasing in both frequency and magnitude in the inland north. Our results highlight that treating the entire Northeast as a uniform hydroclimatic region conceals significant regional variations in extreme discharge trends and, more generally, climate warming will likely increase the sensitivity of historically snowmelt dominated watersheds to extreme precipitation. Understanding this spatial variability in increased extreme precipitation and increased sensitivity to extreme precipitation is crucial for enhancing disaster preparedness and refining water management strategies in affected regions.

1 | Introduction

The frequency of extreme precipitation in the Northeast United States has increased since the late 1990's (Groisman et al. 2005; Kunkel et al. 2010, 2013; Huang et al. 2017; Collins 2019) and is predicted to remain elevated for decades to come (Picard et al. 2023). However, elsewhere it has been observed that the impact of increased extreme precipitation on annual flood maxima has been limited by decreased antecedent soil moisture and changes in snowmelt (Sharma, Wasko, and Lettenmaier 2018; Wasko, Sharma, and Lettenmaier 2019; Wasko and Nathan 2019; Do, Westra, and Leonard 2017), demonstrating that the linkage between increases in extreme precipitation and extreme flooding is modulated by antecedent conditions

and snowmelt dynamics (Armstrong, Collins, and Snyder 2012; Collins et al. 2022; Collins 2019; Wasko, Nathan, and Peel 2020). This linkage is further modulated by the seasonality of the increase in extreme precipitation. For example, Dethier et al. (2020) report that despite an overall increase in the frequency of extreme precipitation in the Northeast U.S., the increase in extreme discharge event frequency has been limited by the lack of an increase in the annual snowmelt peak floods due to early snowpack depletion, which has resulted in an increase in extreme discharge events in the winter season. This effect is likely stronger in the traditionally snowmelt-dominated watersheds in northern latitudes. Furthermore, Huang et al. (2017) argue that the increase in extreme precipitation in the Northeast U.S. is partially driven by increases in extreme precipitation in the fall and climate models indicate a shift in the timing of extreme precipitation from summer and early autumn toward late autumn and early winter (Marelle et al. 2018) should continue for the rest of this century. However, Collins (2019) found that, to date, in the majority of the Northeast U.S. watersheds they analysed, the increase in Northeast U.S. flood counts per year was driven mostly by an increase in the number of June–October floods rather than an increase in late autumns and early winter. Furthermore, Frei, Kunkel, and Matonse (2015) noted that the seasonality of extreme discharge is decoupled from that of extreme precipitation; larger precipitation events during the warm season disproportionately influence trends in extreme precipitation, whereas the magnitude of extreme streamflow is more significant in the cold season, resulting in less pronounced and less spatially coherent trends in streamflow. Thus, while shifts in flood timing are known to have possibly large impacts on water supplies (Barnett, Adam, and Lettenmaier 2005), agricultural productivity (Klaus et al. 2016) and ecosystems (Diehl et al. 2018), significant uncertainty remains in our understanding of how the changes in the frequency and seasonality extreme precipitation may drive possible changes in extreme flooding in the Northeastern U.S. and other regions where extreme precipitation is increasing.

Additionally complicating the linkage between extreme precipitation and flooding in the Northeast U.S., consistent with Collins' (2019) identification of a coastal influence on extreme discharges, Armstrong, Collins, and Snyder (2014) found that in this region coastal low pressure systems are associated with higher magnitude flood events near the coast. Picard et al. (2023), however, report that extreme precipitation is projected to increase most in inland regions. In an analysis of flood seasonality across the contiguous United States, Villarini (2016) highlighted the spatial incoherence in the Northeast, revealing stronger seasonality in inland, northern regions and weaker seasonality in the southern, coastal areas. The effects of latitude and coastal proximity on the spatial variations in changes in extreme discharge thus remain poorly understood.

Finally, the linkage between extreme precipitation and flooding in the Northeastern U.S. is further complicated in part because ~25% of the increase in regional extreme precipitation is associated with frontal systems that may produce locally intense downpours (Huang, Winter, and Osterberg 2018). Such events may only produce extreme discharges on small watersheds, as larger watersheds would integrate flows from many smaller watersheds outside the localised region of extreme precipitation. Even tropical cyclones–which impact large regions–produce pockets of highly localised rainfall (Avila and Cangialosi 2011). Thus, even cyclones, which Huang, Winter, and Osterberg (2018) argue contribute about 50% to the recent increase in extreme precipitation, may preferentially drive extreme discharge in smaller watersheds, introducing a watershed scale component to the linkage between extreme precipitation and flooding.

In sum, the impacts of the well documented increase in extreme precipitation in the Northeast U.S. on extreme flooding are likely modulated by the seasonality of changes in extreme precipitation and watershed size, latitude and distance from the coast. It follows that any impacts of changes in extreme precipitation on extreme flooding vary spatially. Thus, grouping northern and southern and coastal and inland regions into a single region may mask any linkages between changes in precipitation and flooding, limiting our ability to generalise our understanding of the linkages between changes in extreme precipitation and flooding. As a first step toward unravelling this spatial variation, Collins (2019) analysed flood modality and timing in the Northeast U.S. to identify specific flood types and their distribution. Building on this work, here we seek to advance beyond classification to address the broader spatial and seasonal trends governing changes in extreme flooding in the Northeastern U.S. and its evolution over time. To help constrain future scenarios, this research has three key research questions: (a) How do coastal proximity and latitude impact the linkage between extreme precipitation and extreme discharge? (b) Is there spatial variation in how documented changes in the frequency and magnitude of cold season (Nov–May) extreme discharges (Dethier et al. 2020) compare to changes during the warm season (June–Oct)? (c) Do variations in drainage area control the timing and magnitude of extreme discharges, and if so, in what seasons and regions? Through these efforts, we seek greater understanding of changes in the spatial and temporal distribution of extreme discharges, understanding critical for adapting to the evolving hydroclimatic conditions in the Northeast U.S. and other regions where extreme precipitation is increasing.

2 | Data And Methods

2.1 | Study Area

The study region shown in Figure 1 aligns with that used by Huang et al. (2017), Huang, Winter, and Osterberg (2018), Frei, Kunkel, and Matonse (2015) and Walsh et al. (2014). Following the methodology of Wasko, Nathan, and Peel (2020), we conducted distinct analyses of regions within our study area that exhibit similar seasonality traits. Guided by regression model outcomes for extreme precipitation and discharge seasonality, as well as previous findings on hydroclimatic variations between coastal and inland areas (Magilligan and Graber 1996; Armstrong, Collins, and Snyder 2014; Collins 2019; Picard et al. 2023), we segmented the study area into four quadrants. The quadrants are approximately equally divided north and south of the 42° latitude line and, somewhat arbitrarily, within and beyond 150 km from the coast. The selection of the 150 km buffer to define the coastal region was guided by the spatial trends we observed in the extreme precipitation and discharge seasonality data (see below) and chosen to be large enough to ensure a sufficient number of gages in the coastal regions.

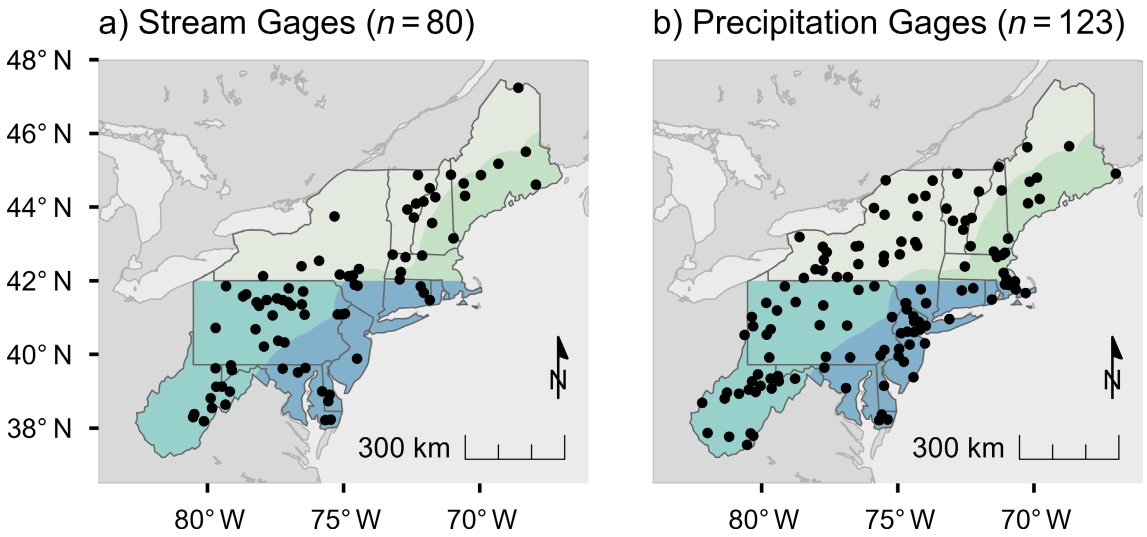

FIGURE 1 | Study area map, including the (a) HCDN USGS stream gages and (b) GHCNd precipitation gages used for analysis. The study area is broken into quadrants, defined North and South of 42° N and within and beyond 150 km from the coast.

Similarly, we followed Huang et al. (2017) and defined extreme precipitation events for a given station as those days with the top 1% of daily precipitation depths among wet days across the entire precipitation record. Wet days are defined as recording greater than 0.254 mm of precipitation. From this subset of precipitation depths, for each year of record we determined the total amount of extreme precipitation. Daily precipitation depths were extracted from the NOAA Global Historical Climatology Data Network daily (GHCNd) dataset, a compilation of quality-assured daily climate records worldwide. Within the Northeast, we identified 123 stations with a sufficiently complete (at least 80%) daily precipitation record spanning from 1901 to 2023, following Huang et al.'s record completeness criteria. Precipitation data were analysed across two time intervals, first across the entire record and then, to match discharge records, across the period spanning 1950–2023. The top 1% of wet days threshold resulted in an average of 1.25 extreme precipitation events per GHCNd station per year. A total daily precipitation depth of 37.3 mm (1.47 in.) was the lowest amount to qualify as extreme precipitation (top 1% wet day), however the exact threshold depth varies from station to station.

We examined changes in extreme discharges in the Northeast using daily records from stream gages within the USGS Hydro-Climatic Data Network 2009 (HCDN). Unlike Villarini (2016), we only considered unregulated, non-urbanised streams. The HCDN comprises streams with minimal anthropogenic impact (U.S. Geological Survey 1994), updated most recently in 2009. Unless otherwise noted, discharges are mean daily discharges. While defining extreme discharge events based on instantaneous (rather than mean daily) discharge would have been preferred, instantaneous peak discharge records lack sufficient length for analysing temporal trends. Published USGS annual peaks series only include one flow per year and are thus inadequate for analyses of trends in seasonality. From the HCDN, we identified 80 gages in the Northeast with records spanning 1950–2023. Given that discharge records are not as extensive as precipitation records, we chose the starting year of 1950 to balance record length and the number of gages. Extreme discharge events were identified based on the top 10% of peak daily discharges for a given stream gage. The detailed selection criteria are described below. To standardise the comparison across watersheds of different areas, we normalised all extreme discharge events (calculated from mean daily discharges) by the 2-year flood (Q_2) at their respective stream gages. Consistent with the traditional determination of Q_2, the magnitude of the 2-year-flood was determined using the Log-Pearson Type III distribution fit to annual instantaneous peak discharges.

2.2 | Changepoint Analysis

2.2.1 | Extreme Precipitation

To determine gridded spatial averages of extreme precipitation across the Northeast, we followed the methodology of Huang et al. (2017). Briefly, we split the study area into a 1° latitude by 1° longitude grid and found the average annual depth of extreme precipitation for each station within a grid cell. We then averaged these grid averages across all cells to find a single spatially averaged extreme precipitation depth across the Northeast for each year. Using the time series of spatially averaged extreme precipitation depths, we identified the year if and when a significant change occurred in mean annual extreme precipitation using the 'changepoint' package (Killick & Eckley, 2014) in (R Core Team, 2024), which conducts changepoint analysis based on the methodology of Hinkley (1970). Although we include an additional 9 years of recent data, our results are consistent with Huang et al. (2017) in identifying a changepoint year of 1996 across the entire study area. Post-1996, there was a notable increase in extreme precipitation, with this increase being statistically significant ($p = 0.0001$) using Welch's t-test. To capture the diverse hydroclimatology within the Northeast, we recalculated the spatially averaged total annual extreme precipitation for each quadrant and then assessed changes across the 1996 changepoint for each quadrant individually. To evaluate more recent changes, we compared extreme precipitation between the historical period (pre-1996) and the most recent decade (2014–2023) using Welch's t-test.

2.2.2 | Extreme Discharge

Defining 'extreme' discharge requires more nuance, as stream discharge is continuous with high discharges from a single event possibly spanning multiple days. To avoid this issue, we used the 'peaks' function from the *R* package 'splus2R' (Constantine & Hesterberg, 2024) to identify a peak as having the maximum discharge centered over a running 7-day window (Figure 2). With the peak flows identified and multi-day events removed, we then considered various thresholds for extreme discharge, including the top 1%, top 5% and top 10% peak flow events for each gage. There were too few top 1% events to determine their spatial variation, while the top 5% and top 10% of all events generally yielded similar results. Hence, we considered the top 10% peak flow events to ensure robustness of the spatial analyses. The top 10% of peaks typically resulted in about 3–4 extreme discharge events for each gage per year, generally consistent with Collins' 'peak over threshold' classification for extreme discharges in the Northeast (Collins 2019).

Following the methodology used for extreme precipitation, for the extreme discharge changepoint analyses only, the normalised extreme discharges were summed for each year. We also applied the same spatial averaging used for extreme precipitation to extreme discharge, summing the normalised annual extreme discharge for each stream gage and finding the gridded and regional averages for each year.

2.3 | Seasonality

Following Magilligan and Graber (1996), we used circular statistics to examine the changes in flood seasonality. To employ this technique, we first converted days of the year (j) to radians (θ).

$$\theta = 360 \cdot \left(\frac{j}{365}\right) \cdot \left(\frac{\pi}{180}\right) \tag{1}$$

By averaging over the n extreme events in a given region we used the mean resultant length ($\overline{R}$) to convey the seasonality of flood events and the vector mean ($\overline{\theta}$) to express the mean date of flood events. $\overline{R}$ is a measure of unimodality, with higher $\overline{R}$ indicating more unimodal flood seasonality.

$$\overline{\theta} = \text{atan2}\left(\frac{1}{n}\sum_{i=1}^{n}\sin(\theta_i), \frac{1}{n}\sum_{i=1}^{n}\cos(\theta_i)\right) \tag{2}$$

$$\overline{R} = \sqrt{\left(\frac{1}{n}\sum_{i=1}^{n}\sin(\theta_i)\right)^2 + \left(\frac{1}{n}\sum_{i=1}^{n}\cos(\theta_i)\right)^2} \tag{3}$$

We calculated $\overline{R}$ and $\overline{\theta}$ for each HCDN stream gage and GHCNd precipitation gage. This process was carried out for all years (1950–2023) and separately for the subsets of years before and after the 1996 extreme precipitation changepoint. We then used a multiple regression model to compare these circular statistics to the geographic characteristics of each gage, specifically latitude, coastal proximity, elevation and the drainage area. Furthermore, we computed $\overline{R}$ and $\overline{\theta}$ for both extreme precipitation and extreme discharge across each of the four quadrants.

We tested changes in seasonality using the Cox–Lewis statistic (Dethier et al. 2020; Cox and Lewis 1966). The Cox–Lewis statistic calculates a Z-score by assessing how observed events in a time series deviate from the expected distribution.

$$Z = \frac{1}{n}\sum_{i=1}^{n}\frac{(t_i - t_m)}{\frac{t_l}{\sqrt{12\pi}}} \tag{4}$$

where t_i is the year of each extreme discharge event. The midpoint year, denoted as t_m, is determined as the median year between the start and end of the record. Additionally, t_l indicates the length of the record in years. A positive Z score indicates an increase in frequency over time, while a negative Z score denotes a decrease.

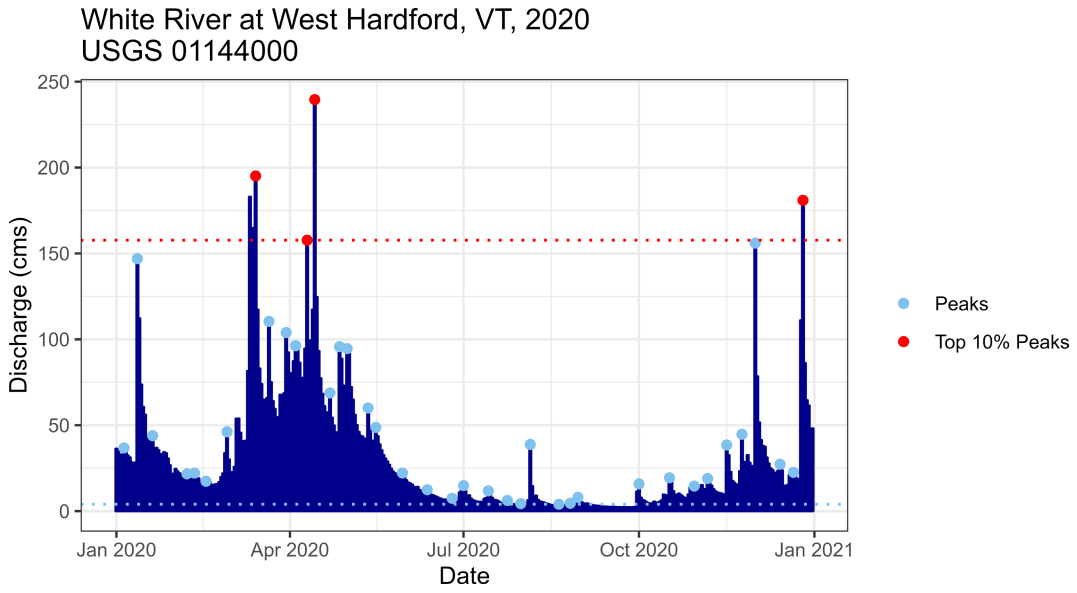

FIGURE 2 | Peak discharges for Vermont's White River, 2020. Weekly peak discharges are shown in blue. The top 10% of these peak flows, shown in red, are selected as extreme discharge events for use in this study.

We computed Cox–Lewis Z scores to evaluate extreme discharge events at each gage. Subsequently, we categorised each extreme discharge event into a 'cold' season (November to May) and 'warm' season (June to October), following a seasonal designation similar to Collins (2019). We calculated the Cox–Lewis statistic separately for the cold and warm seasons. This seasonal breakdown is valuable for distinguishing floods influenced by snowmelt that occur in the cold season (November to May) from those unaffected by snowmelt that occur in the warm season (June to October) and may experience influence from tropical cyclones. Using a multiple regression model we compared these Cox–Lewis statistics with latitude, coastal proximity, elevation and drainage area.

Finally, we assessed changes in flood magnitude over time within the warm and cold seasons. We identified the largest normalised extreme discharge event within each quadrant for both the warm and cold seasons. We established a linear regression model to examine how these seasonal maximums relate to the year and conducted a t-test on the regression statistic to determine the significance of the slope of seasonal maximums over time.

3 | Results

3.1 | Changepoint Analysis

As noted earlier, although we include an additional 9 years of recent data, our results are consistent with Huang et al. (2017) in identifying for extreme precipitation a changepoint year of 1996 across the entire study area ($p = 0.0001$, Figure 3a). In contrast, across the entire study area there is no significant change point in the extreme discharge record (Figure 3b) despite the upward trend. This discrepancy prompts an exploration into why the strong increase in extreme precipitation in 1996 does not correspond to a similar change in extreme discharge.

Changepoint analysis within each quadrant begins to hint at spatial variability. All quadrants exhibit an increase in extreme precipitation in the post 1996 time period compared to the pre 1996 time period, but this increase is only significant in inland quadrants per Welch's t-test in 1996 (Table 1). Since 1996, however, the quadrants have shown distinct behaviours. In the coastal north, extreme precipitation has trended downwards toward pre-1996 levels (Figure 4b). This slope is statistically significant ($p = 0.017$) per linear regression. The other three quadrants also experience decreasing trends, shown in Figure 4a,c,d, but these slopes are not statistically significant. Furthermore, in a comparison in each quadrant of the most recent decade (2014–2023) of extreme precipitation to pre-1996 levels, only the inland north remains significantly higher than the pre-1996 record (Table 1; Figure 4a). While extreme precipitation did increase everywhere in the Northeast post-1996, that effect has only persisted over Vermont and surrounding regions. These results highlight the insight that is lost when results are averaged over the entire Northeast.

3.2 | Seasonality

Figure 5 shows the distribution of mean resultant length $\overline{R}$ values for both extreme precipitation and discharge across

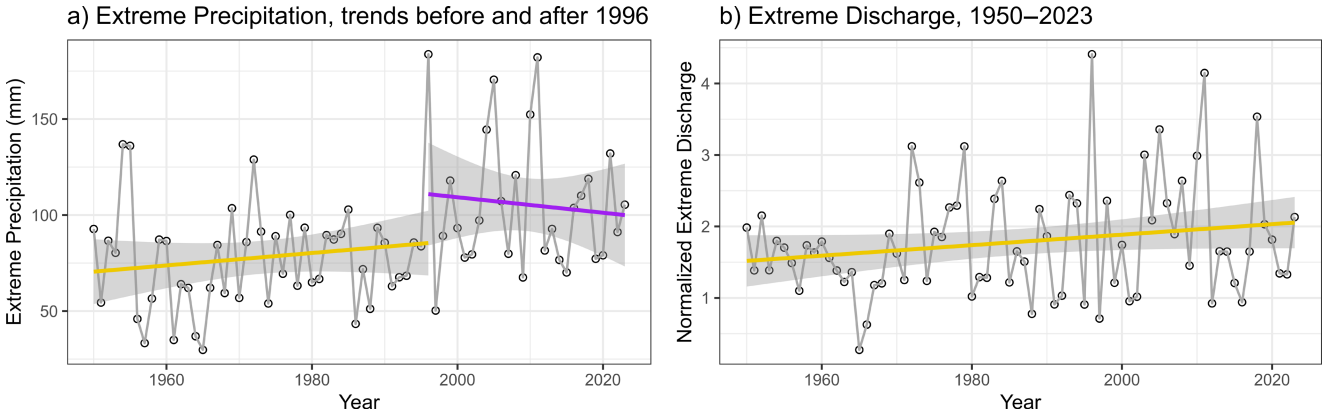

FIGURE 3 | Annual trends in (a) extreme precipitation and (b) extreme discharge across the Northeast. Trendlines are divided at changepoint years. Extreme discharge events are normalised by the 2-year flood at their respective stream gages prior to spatial averaging.

TABLE 1 | p Values from linear regression analysis and Welch's t-test (one-sided, for increase across 1996 changepoint), examining changes in extreme precipitation across the 1996 changepoint in each quadrant.

Test	p, Inland *N.*	p, Coastal *N.*	p, Inland *S.*	p, Coastal *S.*
EP, pre-1996 versus post-1996	4.35×10^{-4}	1.33×10^{-1}	6.50×10^{-3}	1.06×10^{-1}
EP trend, 1996–2024	3.87×10^{-1}	1.70×10^{-2}	1.11×10^{-1}	2.25×10^{-1}
EP, pre-1996 versus post-2014	1.56×10^{-2}	9.83×10^{-1}	2.97×10^{-1}	7.23×10^{-1}
Red: significant, negative				
Blue: significant, positive				

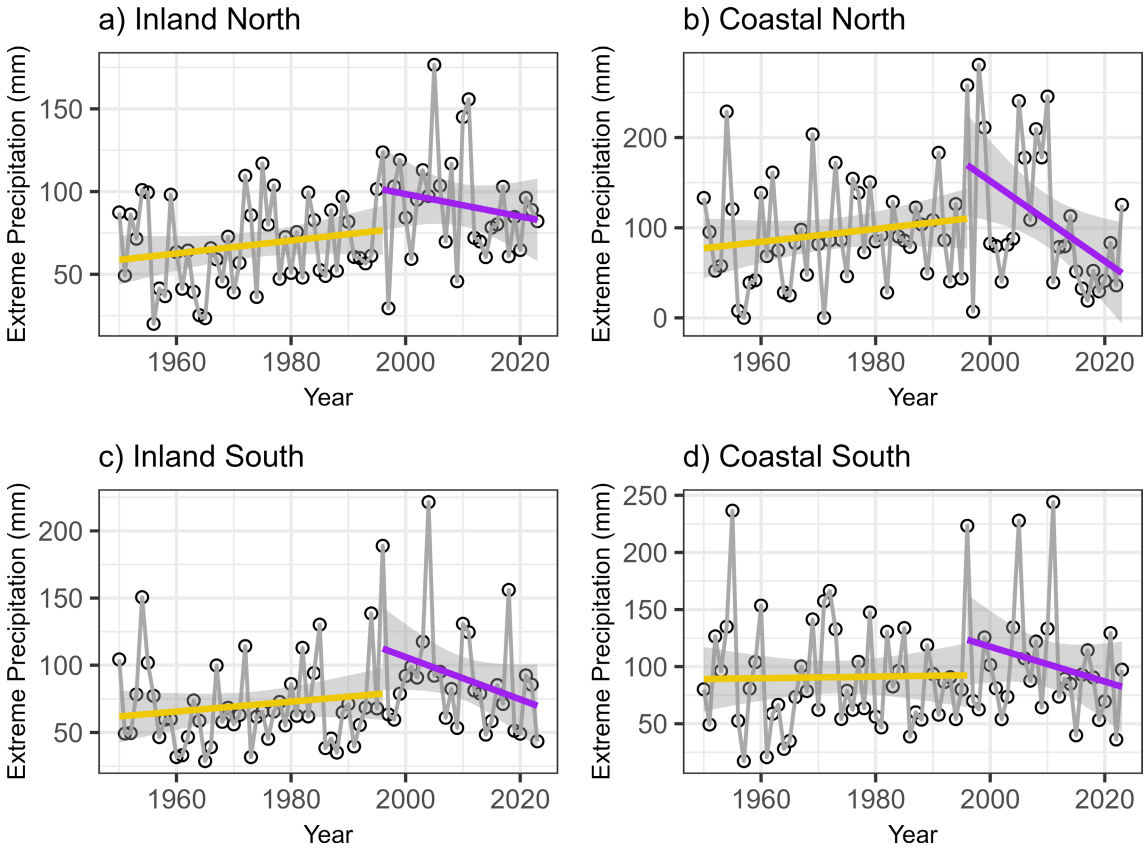

FIGURE 4 | Annual trends in extreme precipitation for each quadrant. Trendlines are divided at the 1996 changepoint.

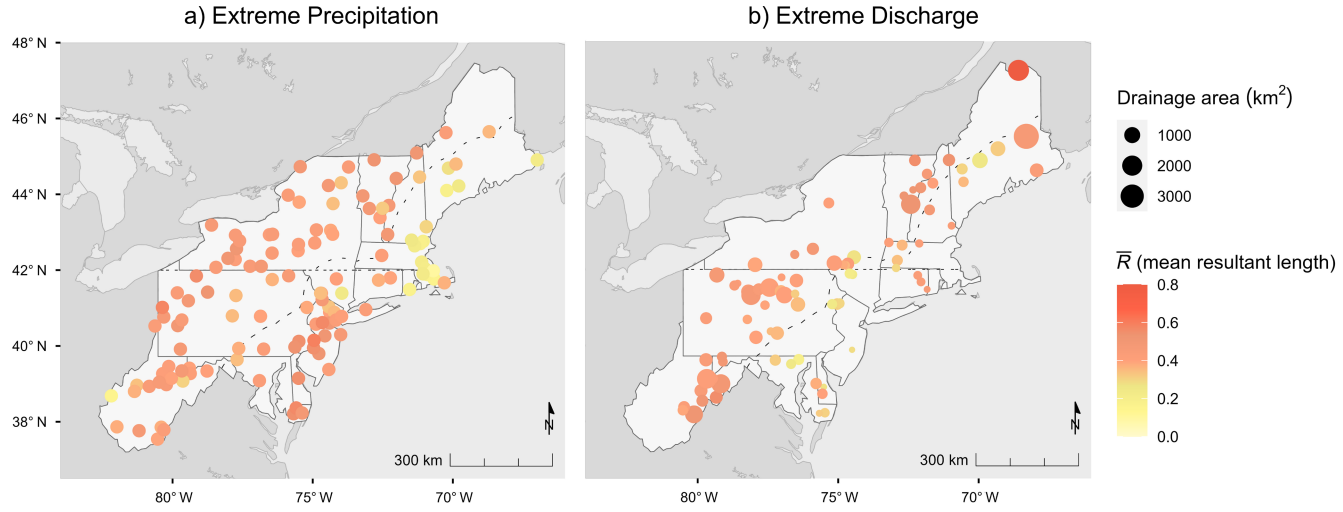

FIGURE 5 | Mean resultant length $\overline{R}$ for (a) extreme precipitation and (b) extreme discharge. Stream gage location points are scaled by drainage area. Dashed lines demarcate quadrant boundaries.

the entire Northeast. The $\overline{R}$ values for extreme precipitation are consistently lower (less unimodal) along the northern coast. Northern coastal regions experience more variable, multimodal seasonality of extreme precipitation. Southern coastal and inland extreme precipitation is more unimodally distributed.

While the coastal effect on the mean resultant length $\overline{R}$ of extreme precipitation is limited to the northern coast, the $\overline{R}$ values for extreme discharges are consistently lower (less unimodal) along both the northern and southern coasts. In Figure 5b, each stream gage location point is scaled by drainage area. Close visual inspection hints at streams with smaller drainage areas having lower $\overline{R}$ values. A quantitative investigation of this trend is presented in Table 2, which shows the results of a multiple regression model in which $\overline{R}$ is the dependent variable and latitude, coastal proximity, elevation and the drainage area are the independent variables. Results are presented for both precipitation

TABLE 2 | Outcomes of multiple regression analyses, examining the influence of various geographic features on the mean resultant length ($\overline{R}$) across all years, pre-changepoint and post-changepoint.

Dependent variable	Latitude	Distance from coast	Elevation	Drainage area
Precipitation $\overline{R}$	*	**	—	NA
Precipitation $\overline{R}$, pre-changepoint	**	*	—	NA
Precipitation $\overline{R}$, post-changepoint	—	**	—	NA
Discharge $\overline{R}$	*	**	—	*
Discharge $\overline{R}$, pre-changepoint	***	*	—	—
Discharge $\overline{R}$, post-changepoint	—	*	—	**
Red: significant negative coefficient	Signif codes: '***' 0.001 '**' 0.01 and '*' 0.05			
Blue: significant positive coefficient	— not significant; 'NA' not applicable			

and discharge $\overline{R}$, across all years and before and after the 1996 extreme precipitation changepoint.

We find a highly significant variation in the mean resultant length $\overline{R}$ of extreme precipitation and distance from the coast. Inland stations consistently have more unimodally distributed extreme precipitation seasonality. This relationship holds true across all years, pre-changepoint and post-changepoint. We also note a latitude effect in the mean resultant length $\overline{R}$ of extreme precipitation. Across the entire period and pre-changepoint, northerly stations exhibit less unimodal extreme precipitation seasonality.

For extreme discharge, $\overline{R}$ holds a significant positive relationship with latitude, distance from the coast and drainage area. Across the entire period record, the distribution of extreme discharges is more unimodal in small, northern, inland watersheds. When subset by changepoint year, before the changepoint year $\overline{R}$ is only significantly correlated with latitude and distance from coast and is independent of watershed size. The opposite occurs post changepoint, i.e., $\overline{R}$ is only significantly correlated with watershed size and independent of latitude and distance from coast.

Understanding the drivers on these changes in $\overline{R}$ motivates a closer investigation of the seasonal distribution of extreme events. The rose diagrams in Figure 6 demonstrate the seasonal distribution of extreme precipitation events for each quadrant. Generally, extreme precipitation events are most common in the summer and fall. Inland regions, particularly the inland north quadrant ($\overline{R}=0.424$), have the most unimodal summer–fall seasonality. Consistent with Figure 5, the coastal north quadrant has the least unimodal seasonal distribution ($\overline{R}=0.224$). Notably, there are more winter and early spring extreme precipitation events in the coastal north.

The inland north quadrant has experienced the most significant and lasting increase in extreme precipitation after the 1996 extreme precipitation changepoint (Figure 4a). Thus, Figure 7 investigates changes in the seasonal distribution of extreme precipitation across this changepoint for the inland north.

$\overline{R}$ and $\overline{\theta}$ do not change significantly across the changepoint in Figure 7 and most seasons experience relative increases in the frequency of extreme precipitation. These increases are strongest in the fall, but the overall seasonal distribution is consistent across the changepoint.

In Figure 8, rose diagrams show the distribution of extreme discharge events about the calendar year. Results are presented for the inland north quadrant and the inland south quadrant, which show the most (inland north) and least (inland south) change in $\overline{R}$ across the 1996 changepoint year, respectively. No quadrants experience a significant change in $\overline{\theta}$ across the changepoint. Historically, watersheds in the southern part of the study area have experienced highly variable flood seasonality (low $\overline{R}$) and that has continued in the regime of modern climate change. Northern regions, however, historically had strongly unimodal flood regimes, concentrated around the spring flood. Changes in seasonality are driven by an increase in flood frequency outside of the spring mode rather than a change in the date of the springmelt flood mode.

In the inland north quadrant, which has the largest changes in seasonality, with $\overline{R}$ values dropping by about 0.18 (Figure 8a), most extreme discharges continue to be associated with the spring melt. However, relative to other seasons, the occurrence of extreme discharge events in the spring has exhibited a declining trend over time. In contrast, extreme discharge events in the summer, fall and winter have seen an increased proportion in the overall distribution.

The inland south also exhibits a relative peak about the spring flood, but this peak is broader and earlier in the year than in the inland north. The changes across the changepoint are less coherent in the inland south quadrant. However, we do note a relative decrease in spring floods and an increase in early fall and early winter floods, similar to the inland north.

Figure 9 presents a summary of changes in the seasonality of extreme discharge across the 1996 changepoint year for all four quadrants. The coastal north and inland north exhibit the greatest changes in $\overline{R}$. Both quadrants are characterised by increases in flooding outside of the historic spring mode. The inland south shows the same decrease in spring floods as the northern regions, but a less consistent response

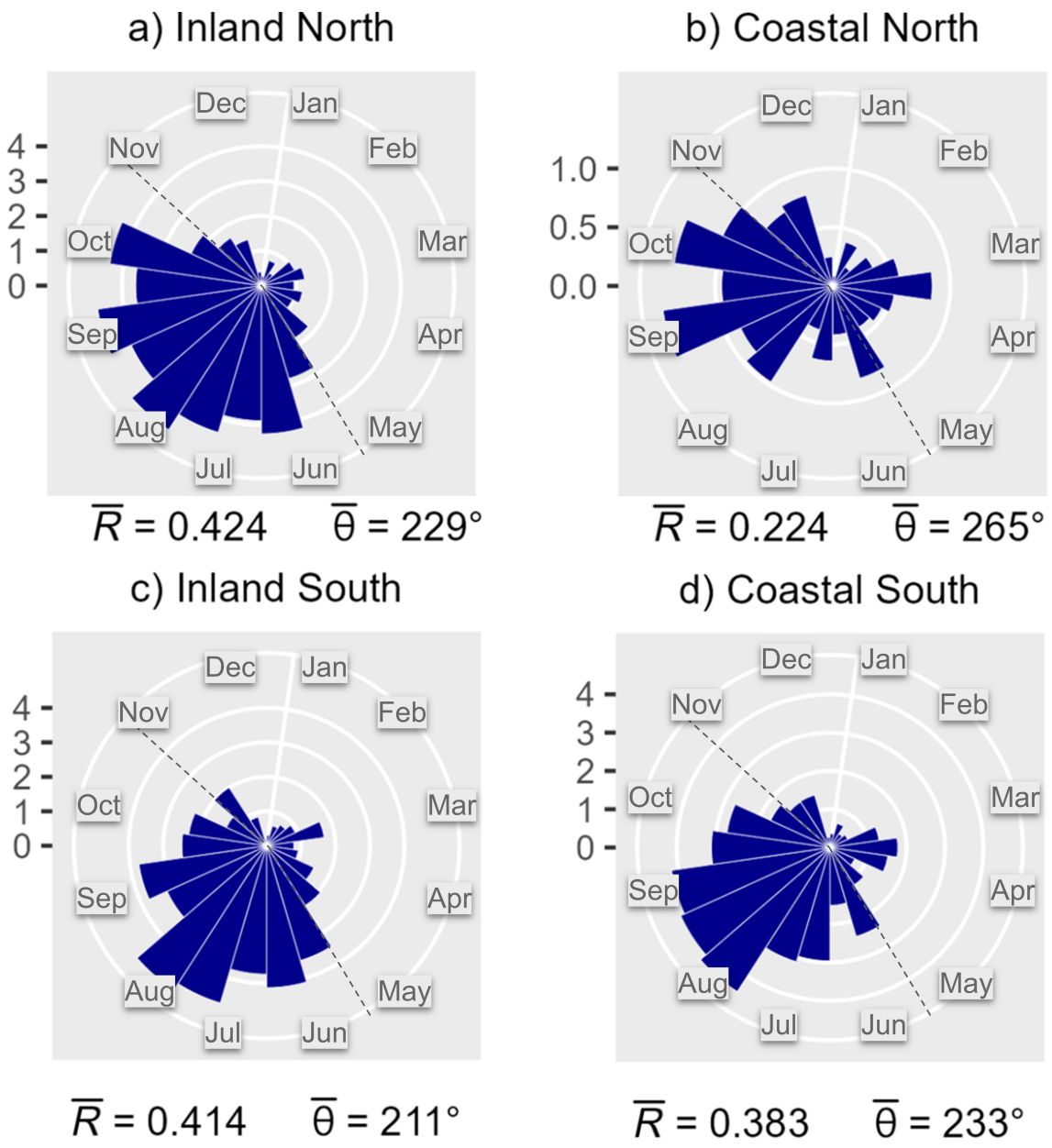

FIGURE 6 | Rose diagrams showing the distribution of extreme precipitation events for each quadrant, across all years 1950–2023. The length of each bar represents the number of events per year within a given quadrant. Warm (June–Oct.) and cold (Nov–May) seasons are split by dashed lines.

throughout the rest of the year. Strong increases are observed for both early fall and early winter extreme discharge events in this quadrant. The coastal south has the lowest historic $\overline{R}$. Nonetheless, we observe a similar decrease in the winter–spring modes in the inland south and relative increases other times of the year–particularly in the fall.

The rose diagrams in Figure 9 demonstrate changes in each season relative to each other. We compare changes in the frequency of extreme discharge events within the warm (June–Oct) and cold (Nov–May) seasons using the Cox–Lewis statistic. Cold season analysis produces insignificant Cox–Lewis *Z* scores, indicating a consistent frequency in cold season extreme discharge events over time. In a multiple regression model, no geographic variables are strong predictors of changes in frequency of extreme discharge across the entire year or the cold season (Table 3).

The warm season, however, exhibits significant positive Cox–Lewis *Z* scores across much of the study area, as seen in Figure 10, indicating an increase in the frequency of warm season floods over time. Furthermore, stream gages with smaller drainage areas appear to have higher Cox–Lewis *Z* scores. In a multiple regression model, there is a significant negative correlation between the Cox–Lewis *Z* score and both drainage area and elevation. Follow-up analyses found no significant interaction between area and elevation. The correlation between the elevation and Cox–Lewis *Z* score is largely driven by high elevation sites in West Virginia, which do not exhibit significant Cox–Lewis *Z* scores. There is a significant positive relationship between the Cox–Lewis *Z* score and latitude. Increases in warm season extreme discharges are favoured in smaller, higher and more northern watersheds (Table 3).

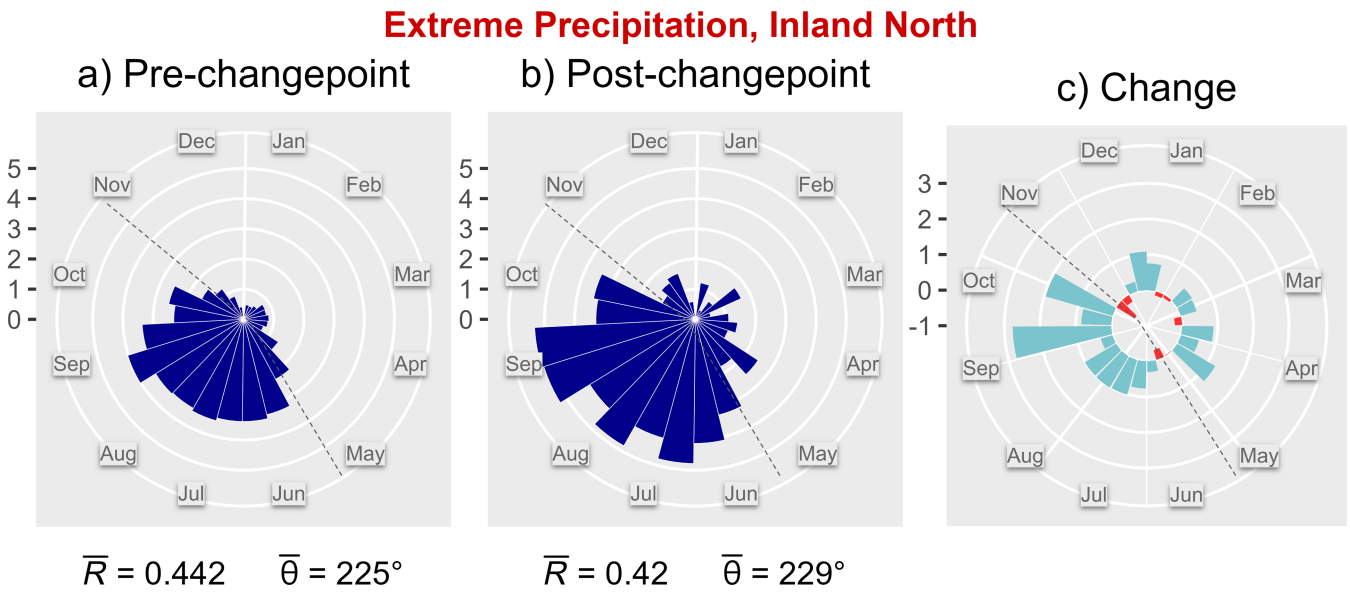

FIGURE 7 | Rose diagrams for the inland north quadrant, showing the distribution of extreme precipitation events for pre-changepoint, post-changepoint and the difference between pre- and post-changepoint. For the change plot, light blue represents an increase in relative frequency and red represents a decrease. The length of each bar represents the number of events per year within a given quadrant. Observations are normalised by the number of years to allow for direct comparison. Warm (June–Oct.) and cold (Nov–May) seasons are split by dashed lines.

Finally, an investigation of changes in extreme discharge magnitude reveals that the sizes of the largest floods in each season are constant with time for most quadrants. The inland north quadrant, however, exhibits a significant trend over time. Figure 11a shows no trend in the size of cold season floods for the inland north quadrant. Warm season floods (Figure 11b), however, exhibit a statistically significant increasing trend ($p = 0.01$) in magnitude. The magnitude of warm season floods is approaching that of the cold season flood, which has historically been higher.

4 | Discussion

4.1 | Spatial Variation in Extreme Discharge

Spatially, the multiple regression results (Table 2) indicate that the seasonality in extreme discharges depends strongly on both coastal proximity and, prior to the 1996 changepoint year, latitude (Figure 5b). Historically, and not surprisingly, with increasing latitude the highest discharges of the year are increasingly associated with snowmelt in the early spring. While precipitation can amplify snowmelt discharges, in general spring snowmelt discharges are asynchronous with extreme precipitation (Figures 6 and 7) and thus extreme discharges in snowmelt dominated watersheds are mostly decoupled from extreme precipitation. Indeed, in the pre-changepoint years, latitude has a positive proportional relationship to extreme discharge seasonality, but a negative proportional relationship to extreme precipitation seasonality (Table 2).

Huang, Winter, and Osterberg (2018) found that about one third of extreme precipitation in the Northeast U.S. is associated tropical cyclones which primarily occur during the early fall. The impacts of tropical cyclones are generally greatest along the coast, as indicated by the significant variation in extreme precipitation with distance from the coast (Table 2). This influence from extreme precipitation results in more uniform extreme discharge seasonality in coastal regions (Figure 5), driving a significant variation in extreme discharge with distance from the coast (Table 2).

Taken together, the above impacts of latitude and distance from the coast align with the earlier findings of Magilligan and Graber (1996), who note a more unimodal spring flood season in inland northerly regions where the fall precipitation mode is less pronounced. These results, driven by spatial heterogeneity in flood mechanisms, highlight that grouping the entire Northeast into a single region hides significant regional variation in extreme discharge trends.

4.2 | Temporal Variation in Extreme Discharge

Although its role is diminishing, across the entire Northeast U.S. the spring season has an historical and continued ability to generate floods, primarily due to the inherent capacity of leaf-off, high soil moisture, low evapotranspiration and snowmelt conditions to generate high flows during this season (Collins 2019). However, consistent with Dethier et al. (2020), we find an increase in early winter season (December and January) extreme discharge in all quadrants (Figure 9). Such early winter high flows are likely driven by an increase in rain events, as opposed to snow, during the early leaf-off period with low evapotranspiration conditions. These flows may be further enhanced by rain on snow or rain on frozen ground. While this increase in early winter season extreme discharge is changing the temporal distribution of cold season extreme discharge, when integrated over the entire cold season there has been no significant change in overall cold season (November–May) extreme discharge frequency in any region (Table 3). Nor is this shift toward increasing extreme discharge in early winter impacting the magnitude of the cold season (November–May) peak discharge (Figure 10).

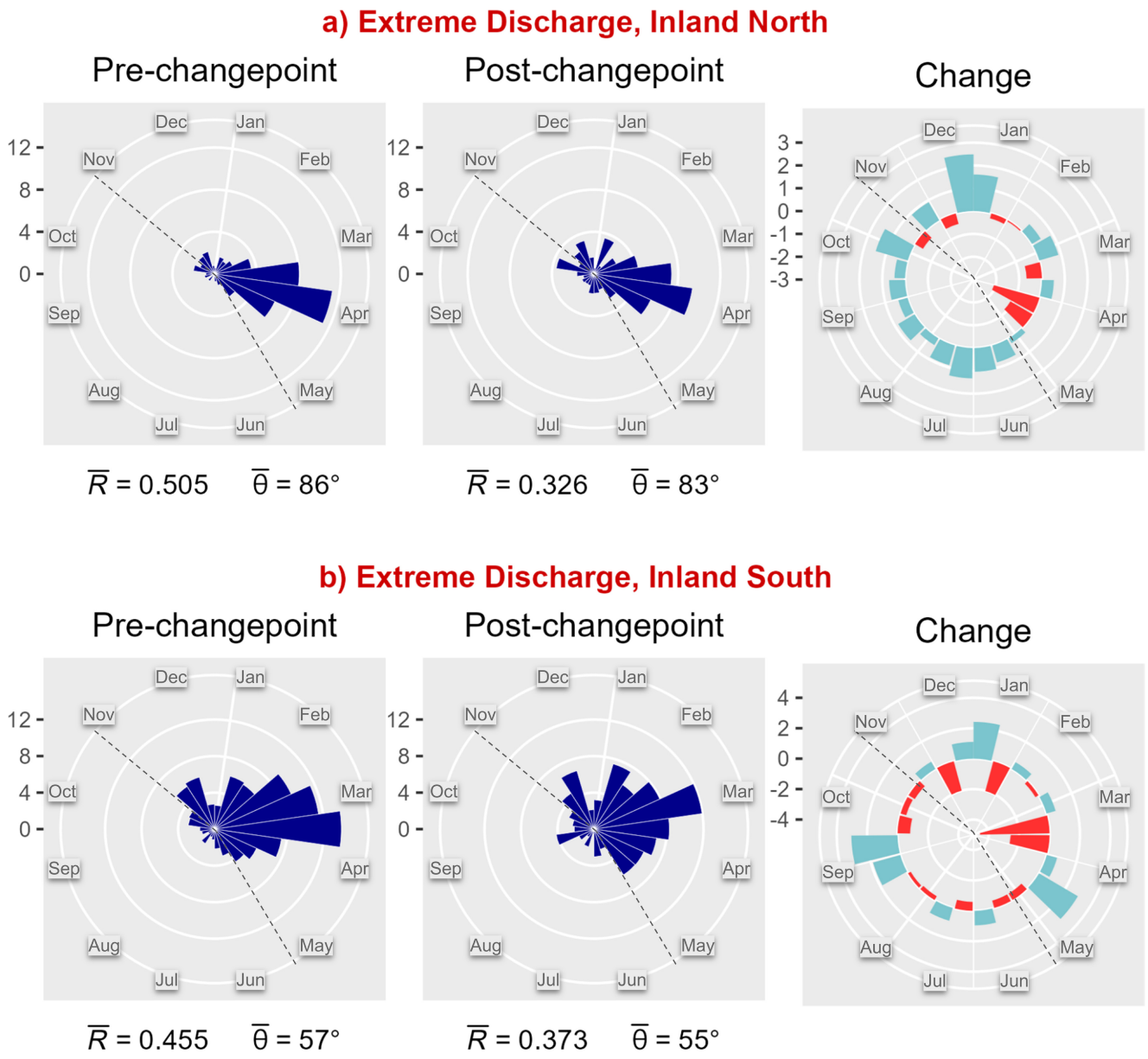

FIGURE 8 | Rose diagrams for the inland north quadrant (a) and inland south quadrant (b), showing the distribution of extreme discharge events for pre-changepoint, post-changepoint and the difference between pre- and post-changepoint. For the change plots, light blue represents an increase in relative frequency and red represents a decrease. The length of each bar represents the number of events per year within a given quadrant. Observations are normalised by the number of years to allow for direct comparison. Warm (June–Oct) and cold (Nov–May) seasons are split by dashed lines.

Historically, snowmelt was more important in generating extreme floods with increasing latitude. As snowmelt floods are largely decoupled from extreme precipitation (Figures 6 and 7), northern regions have historically been buffered against changes in extreme discharges due to changes in extreme precipitation. However, the significant correlation between extreme discharge seasonality and latitude is absent in post-changepoint years (Table 2), hinting at the diminishing, yet still dominant, role of snowmelt discharge in generating extreme discharge in recent decades. As the role of snowmelt has diminished, extreme discharge in northern regions is becoming more sensitive to changes in extreme precipitation. Outside of the spring melt season, floods generated by extreme precipitation are becoming more common. At the same time, extreme precipitation frequency increased across the 1996 changepoint throughout the study area. However, it has remained significantly elevated over 2014–2023 only in the inland north (Figure 4).

This combination of increased sensitivity and continued increased extreme precipitation makes changes in extreme discharges most apparent in the inland north, evidenced by the increasing role of warm season high discharge events in that quadrant (Figure 11). With increasing warming, extreme discharge in northern regions will become increasingly sensitive to changes in extreme precipitation, which in the inland north continues to remain elevated post 1996 with no significant decreasing trend (Figure 4a). Hence, we expect the recent trend of increased extreme discharge in the inland north (i.e., Hurricane

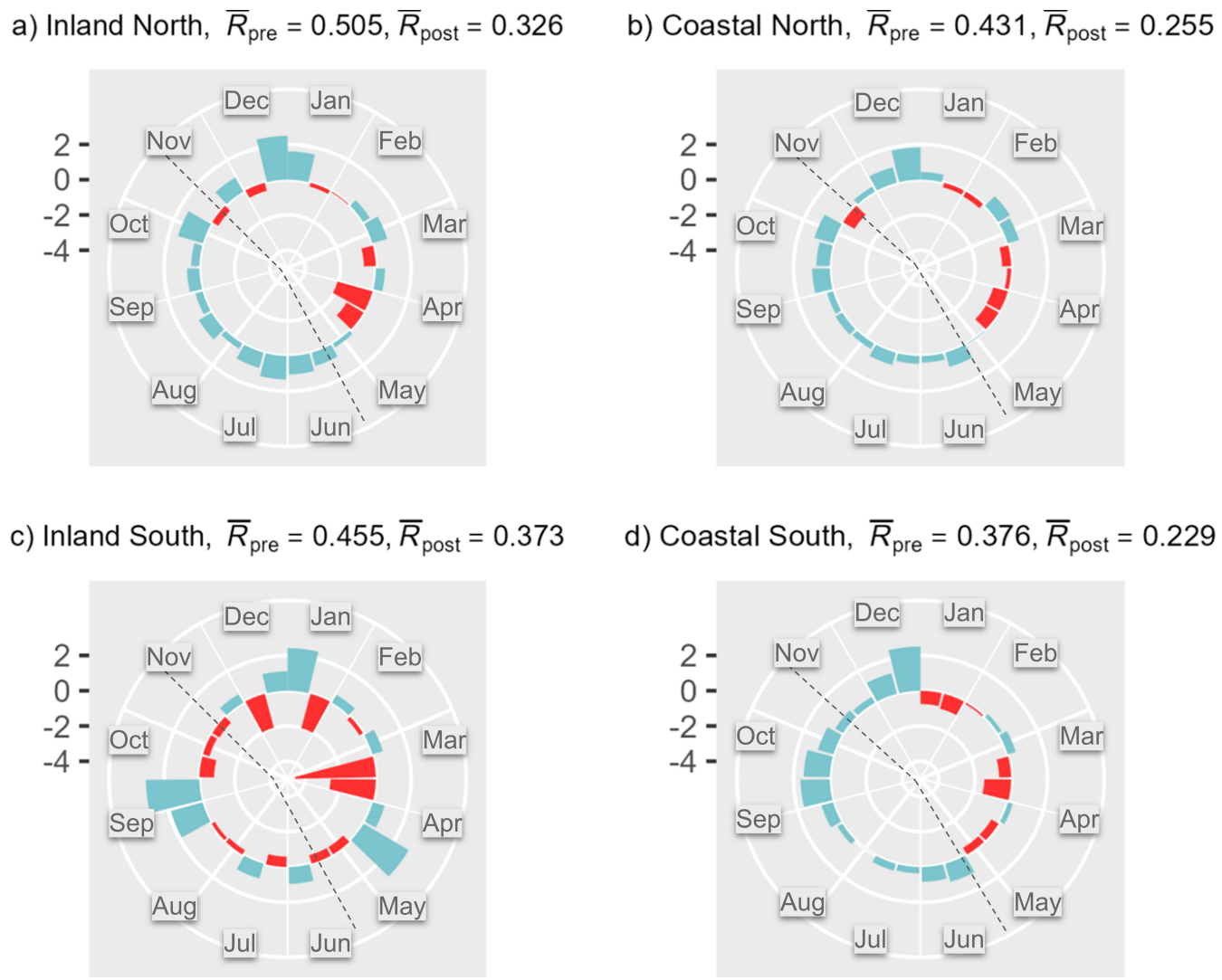

FIGURE 9 | Rose diagrams for all quadrants, showing the difference between pre- and post-1996 distributions of extreme discharge events. Light blue represents an increase in the relative frequency and red represents a decrease. The length of each bar represents the change in the number of events per year within a given quadrant. Observations are normalised by the number of years to allow for direct comparison. Warm (June–Oct) and cold (Nov–May) seasons are split by dashed lines.

TABLE 3 | Outcomes of multiple regression analyses, examining the influence of various geographic features on the Cox–Lewis statistic both throughout the entire year and across seasons.

Dependent variable	Latitude	Distance from coast	Elevation	Drainage area
Discharge Cox–Lewis *Z*, all seasons	—	—	—	—
Discharge Cox–Lewis *Z*, Nov–May	—	—	—	—
Discharge Cox–Lewis *Z*, June–Oct	***	—	*	***
Red: significant negative coefficient		Signif codes: '***' 0.001 '**' 0.01 and '*' 0.05		
Blue: significant positive coefficient		— not significant 'NA' not applicable		

Irene, the 2023 July and December floods) to continue. While the sensitivity of extreme discharge to extreme precipitation is likely also increasing in the coastal north, the amount of extreme precipitation is decreasing there (Figure 4b). Thus, we do not expect extreme discharge frequency to remain elevated for streams in the coastal north.

4.3 | Role of Drainage Area in Modulating Extreme Discharges

Considering the variance in spatial scale between snowmelt-induced flooding and extreme precipitation driven flooding, a significant consequence is the heightened localisation of

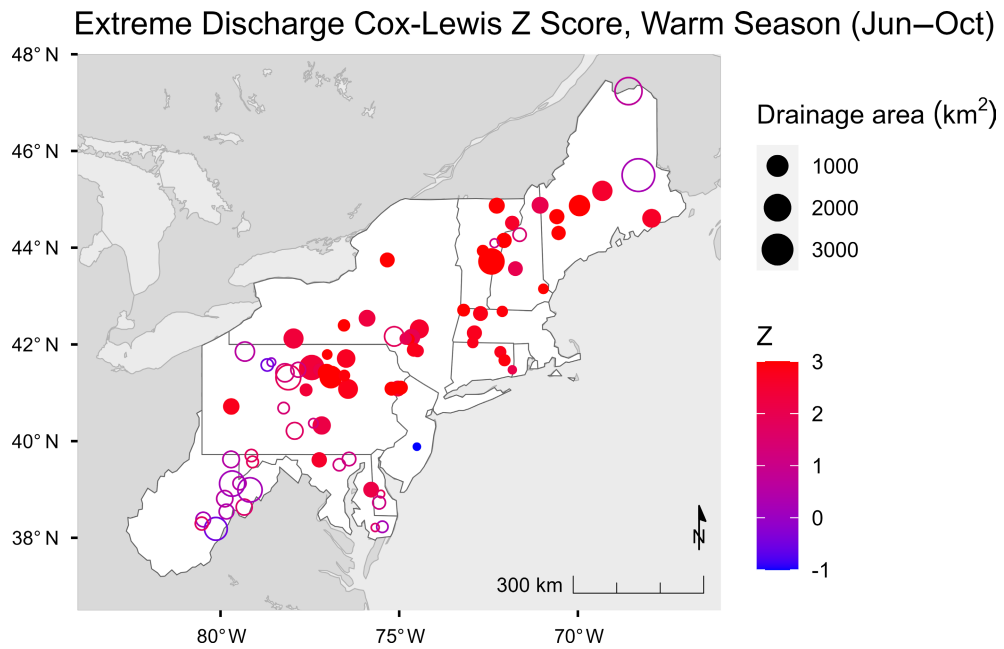

FIGURE 10 | Extreme discharge warm season Cox–Lewis *Z* Scores, points scaled by drainage area. Circles with solid fill are significant ($|Z| > 2$). Dashed lines demarcate quadrant boundaries.

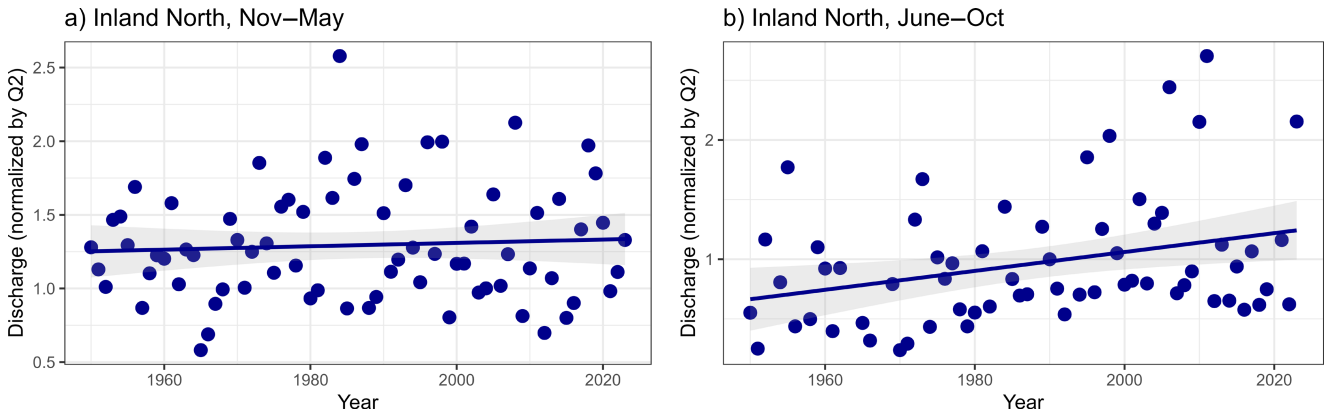

FIGURE 11 | The magnitude of the largest flood in the Inland North region for both the (a) cold and (b) warm seasons over time. Discharges are normalised by Q2 to allow for comparison across streams.

flood impacts through the drainage area effect. Temperature-driven snowmelt events typically impact large regions and can produce high flows in even the largest drainage basins, while extreme precipitation events are more localised and thus primarily affect smaller watersheds. In the inland north, extreme discharge events are increasingly common in watersheds with smaller drainage areas due to a rise in both the frequency of extreme precipitation and sensitivity to extreme precipitation. Before the precipitation changepoint, extreme discharge seasonality ($\overline{R}$) depended on latitude and distance from coast, consistent with influence of coastal storms and inland dominance of springmelt (Table 2). However, post-changepoint, only watershed area is significant, reflecting the decreasing dominance of snowmelt and increasing role of meteorological floods, that is, those due to extreme precipitation events. Since extreme precipitation can be highly localised, meteorological extreme discharges may be increasingly preferentially expressed in smaller watersheds. Small watersheds are responsive to shorter, high intensity precipitation events whereas larger watersheds require longer duration (i.e., spring melt) or larger magnitude (i.e., hurricanes) events and proper antecedent conditions to produce extreme discharge (Knox 1988; Magilligan and Graber 1996; Yellen et al. 2016).

Such changes in $\overline{R}$ are consistent with the observed correlation between changes in warm season extreme discharge and latitude, elevation and drainage area (Table 3). That is, we observe the greatest increase in warm season extreme discharge in smaller, higher and more northern watersheds. Floods in these watersheds were traditionally dominated by springmelt which, as noted above, are mostly decoupled from extreme precipitation. However, inland northern watersheds are increasingly experiencing meteorologically driven (extreme precipitation driven) floods in the warm season. Smaller watersheds are less

likely to have flood mitigation infrastructure such as flood control dams than larger rivers, meaning that increases in flooding in smaller watersheds may pose an outsized risk to the built environment.

5 | Conclusions

The response of extreme discharge events to increasing extreme precipitation varies considerably across the Northeast depending on coastal proximity, latitude and drainage area. We employed changepoint analysis to identify significant shifts in precipitation and discharge patterns and circular statistics to analyse alterations in flood seasonality. Inland regions exhibit a pronounced shift in flood seasonality, especially in the inland north, where extreme discharge events are becoming more frequent outside the traditional spring flood season. Smaller watersheds are experiencing a greater increase in the frequency of warm season extreme discharge events compared to their larger counterparts. Additionally, warm season floods in the inland north are increasing in magnitude, beginning to match or surpass the historically dominant spring floods.

While we observe a change in temporal distribution of cold season extreme discharge, specifically more early winter extreme discharge events, there has been no significant change in overall frequency of cold season extreme discharge across the extreme precipitation changepoint year nor a change in the magnitude of annual peak cold season discharge. Across the entire Northeast U.S. region there has been a significant increase in warm season extreme discharge frequency. The increase in warm season extreme discharge is most pronounced in smaller, inland and more northern watersheds, which were traditionally dominated by springmelt extreme discharges. This shift is consistent with a decreasing dominance of springmelt, especially in inland north and the increasing importance of warm season extreme precipitation events in generating warm season floods. Since extreme precipitation can be localised, this trend is preferentially expressed in smaller watersheds, especially in the inland north where we see corresponding increases in warm season precipitation.

These results highlight the need for developing region-specific adaptation strategies that are tailored to local geographic conditions, especially for regions where historically snowmelt has been the dominant driver of flooding. Our findings show that these regions are likely becoming more sensitive to changes in extreme precipitation. Such increased sensitivity could exacerbate trends in extreme discharge, further highlighting the need for localised climate adaptation strategies (Mach and Siders 2021).

Beyond managing flood risks, changes to the extreme discharge regime affect sediment transport, ecosystems and channel recovery. Changes in flood frequency, magnitude and seasonality may significantly impact macroinvertebrate communities and broader ecosystem health (Diehl et al. 2018; Milner et al. 2013; Robinson, Siebers, and Ortlepp 2018). These alterations disrupt established patterns, potentially leading to mismatches in ecological timing that affect food webs and species survival. In addition, shifts in the flood regime likely impact the ability of channels to recover from disturbances. Thus, human intervention in stream restoration is also affected by alterations to the flood regime. Thoughtful restoration efforts should consider local changes in flood seasonality, frequency and magnitude in order to support the resilience of fluvial ecosystems against future environmental changes.

Acknowledgements

This work was partially funded by the National Science Foundation (BCS-1626414 and BCS-1951469), the Mellam Family Foundation Research Award, the Neukom Institute for Computational Science and the Dartmouth College Department of Earth Sciences. The paper also benefitted enormously from comments from two anonymous reviewers.

Data Availability Statement

GHCNd station precipitation data are available at ftp://ftp.ncdc.noaa.gov/pub/data/ghcn/daily/. Stream gauging records are available at https://waterdata.usgs.gov/nwis (USGS). *R* scripts and supporting materials can be found in a GitHub repository (https://github.com/richardson-owen/EQ_seasonality_NE).

References

Armstrong, W. H., M. J. Collins, and N. P. Snyder. 2012. "Increased Frequency of Low-Magnitude Floods in New England 1." *JAWRA Journal of the American Water Resources Association* 48, no. 2: 306–320.

Armstrong, W. H., M. J. Collins, and N. P. Snyder. 2014. "Hydroclimatic Flood Trends in the Northeastern United States and Linkages With Large-Scale Atmospheric Circulation Patterns." *Hydrological Sciences Journal* 59, no. 9: 1636–1655.

Avila, L. A., and J. Cangialosi. 2011. *Tropical Cyclone Report: Hurricane Irene*, 45. Miami, FL: National Hurricane Center.

Barnett, T. P., J. C. Adam, and D. P. Lettenmaier. 2005. "Potential Impacts of a Warming Climate on Water Availability in Snow-Dominated Regions." *Nature* 438, no. 7066: 303–309.

Collins, M. J. 2019. "River Flood Seasonality in the Northeast United States: Characterization and Trends." *Hydrological Processes* 33, no. 5: 687–698.

Collins, M. J., G. A. Hodgkins, S. A. Archfield, and R. M. Hirsch. 2022. "The Occurrence of Large Floods in the United States in the Modern Hydroclimate Regime: Seasonality, Trends, and Large-Scale Climate Associations." *Water Resources Research* 58, no. 2: e2021WR030480.

Constantine, W., and T. Hesterberg 2024. Splus2R: Supplemental S-PLUS Functionality in R (Version 1.3-5). CRAN. https://CRAN.R-project.org/package=splus2R.

Cox, D. R., and P. A. Lewis. 1966. "The Statistical Analysis of Series of Events."

Dethier, E. N., S. L. Sartain, C. E. Renshaw, and F. J. Magilligan. 2020. "Spatially Coherent Regional Changes in Seasonal Extreme Streamflow Events in the United States and Canada Since 1950." *Science Advances* 6, no. 49: eaba5939.

Diehl, R. M., A. C. Wilcox, D. M. Merritt, D. W. Perkins, and J. A. Scott. 2018. "Development of an Eco-Geomorphic Modeling Framework to Evaluate Riparian Ecosystem Response to Flow-Regime Changes." *Ecological Engineering* 123: 112–126.

Do, H. X., S. Westra, and M. Leonard. 2017. "A Global-Scale Investigation of Trends in Annual Maximum Streamflow." *Journal of Hydrology* 552: 28–43.

Frei, A., K. E. Kunkel, and A. Matonse. 2015. "The Seasonal Nature of Extreme Hydrological Events in the Northeastern United States." *Journal of Hydrometeorology* 16, no. 5: 2065–2085.

Groisman, P. Y., R. W. Knight, D. R. Easterling, T. R. Karl, G. C. Hegerl, and V. N. Razuvaev. 2005. "Trends in Intense Precipitation in the Climate Record." *Journal of Climate* 18, no. 9: 1326–1350.

Hinkley, D. V. 1970. "Inference About the Change-Point in a Sequence of Random Variables." *Biometrika* 57: 1–17.

Huang, H., J. M. Winter, and E. C. Osterberg. 2018. "Mechanisms of Abrupt Extreme Precipitation Change Over the Northeastern United States." *Journal of Geophysical Research: Atmospheres* 123, no. 14: 7179–7192.

Huang, H., J. M. Winter, E. C. Osterberg, R. M. Horton, and B. Beckage. 2017. "Total and Extreme Precipitation Changes Over the Northeastern United States." *Journal of Hydrometeorology* 18, no. 6: 1783–1798.

Killick, R., and I. A. Eckley. 2014. "Changepoint: An R Package for Changepoint Analysis." *Journal of Statistical Software* 58, no. 3. https://doi.org/10.18637/jss.v058.i03.

Klaus, S., H. Kreibich, B. Merz, B. Kuhlmann, and K. Schröter. 2016. "Large-Scale, Seasonal Flood Risk Analysis for Agricultural Crops in Germany." *Environmental Earth Sciences* 75: 1–13.

Knox, J. C. 1988. "Climatic Influence on Upper Mississippi Valley Floods."In *Flood Geomorphology*, edited by V. R. Baker, R. C. Kochel, and P. C. Patton, 279–300. New York, NY: John Wiley and Sons.

Kunkel, K. E., D. R. Easterling, D. A. Kristovich, B. Gleason, L. Stoecker, and R. Smith. 2010. "Recent Increases in US Heavy Precipitation Associated With Tropical Cyclones." *Geophysical Research Letters* 37, no. 24, L24706.

Kunkel, K. E., T. R. Karl, H. Brooks, et al. 2013. "Monitoring and Understanding Trends in Extreme Storms: State of Knowledge." *Bulletin of the American Meteorological Society* 94, no. 4: 499–514. https://doi.org/10.1175/bams-d-11-00262.1.

Mach, K. J., and A. R. Siders. 2021. "Reframing Strategic, Managed Retreat for Transformative Climate Adaptation." *Science* 372, no. 6548: 1294–1299.

Magilligan, F. J., and B. E. Graber. 1996. "Hydroclimatological and Geomorphic Controls on the Timing and Spatial Variability of Floods in New England, USA." *Journal of Hydrology* 178, no. 1–4: 159–180.

Marelle, L., G. Myhre, Ø. Hodnebrog, J. Sillmann, and B. H. Samset. 2018. "The Changing Seasonality of Extreme Daily Precipitation." *Geophysical Research Letters* 45, no. 20. https://doi.org/10.1029/2018gl079567.

Milner, A. M., A. L. Robertson, M. J. McDermott, M. J. Klaar, and L. E. Brown. 2013. "Major Flood Disturbance Alters River Ecosystem Evolution." *Nature Climate Change* 3, no. 2: 137–141.

Picard, C. J., J. M. Winter, C. Cockburn, et al. 2023. "Twenty-First Century Increases in Total and Extreme Precipitation Across the Northeastern USA." *Climatic Change* 176, no. 6: 1–26.

R Core Team. 2024. *R: A Language and Environment for Statistical Computing*. R Foundation for Statistical Computing. https://www.R-project.org/.

Robinson, C. T., A. R. Siebers, and J. Ortlepp. 2018. "Long-Term Ecological Responses of the River Spöl to Experimental Floods." *Freshwater Science* 37, no. 3: 433–447.

Sharma, A., C. Wasko, and D. P. Lettenmaier. 2018. "If Precipitation Extremes Are Increasing, Why Aren't Floods?" *Water Resources Research* 54, no. 11: 8545–8551. https://doi.org/10.1029/2018wr023749.

U.S. Geological Survey. 1994. Hydro-Climatic Data Network (HCDN) -- A USGS Streamflow Data Set for the U.S. for the Study of Climate Fluctuations [Data set]. U.S. Geological Survey. https://doi.org/10.5066/P9HP0WFJ.

Villarini, G. 2016. "On the Seasonality of Flooding Across the Continental United States." *Advances in Water Resources* 87: 80–91.

Walsh, J., D. Wuebbles, K. Hayhoe, et al. 2014. "Our Changing Climate." In *Climate Change Impacts in the United States: The Third National Climate Assessment*, 19–67. Washington, DC: US Global Change Research Program.

Wasko, C., and R. Nathan. 2019. "Influence of Changes in Rainfall and Soil Moisture on Trends in Flooding." *Journal of Hydrology* 575: 432–441.

Wasko, C., R. Nathan, and M. C. Peel. 2020. "Changes in Antecedent Soil Moisture Modulate Flood Seasonality in a Changing Climate." *Water Resources Research* 56, no. 3: e2019WR026300.

Wasko, C., A. Sharma, and D. P. Lettenmaier. 2019. "Increases in Temperature Do Not Translate to Increased Flooding." *Nature Communications* 10: 5676. https://doi.org/10.1038/s41467-019-13612-5.

Yellen, B., J. D. Woodruff, T. L. Cook, and R. M. Newton. 2016. "Historically Unprecedented Erosion From Tropical Storm Irene due to High Antecedent Precipitation." *Earth Surface Processes and Landforms* 41, no. 5: 677–684.